Effect of Pintle Injector Element Geometry on Combustion in a Liquid Oxygen/Liquid Methane Rocket Engine

Brunno B. Vasques[*][†] *and Oskar J. Haidn*[*]
[*]*Technische Universität München*
Boltzmannstr. 15, D-85748 Garching b. München, Germany
brunno.vasques@ltf.mw.tum.de · oskar.haidn@ltf.mw.tum.de
[†]Corresponding author

Abstract

Liquid oxygen and liquid methane are leading options for space propulsion systems requiring high propellant bulk density, good thermal management characteristics and low-toxicity. For the majority of applications, the benefit resulting from smaller tanks and low boil-off losses counterweight any disadvantage in terms of theoretical specific impulse, for instance if compared to the liquid oxygen/liquid hydrogen combination. With respect to mission requirements, of particular interest are those involving planetary landing and orbit manoeuvres, which usually impose a degree of thrust modulation capability over the propulsion system. Strictly from the standpoint of the injection system, the pintle injector is a common choice in this case, due to its inherent combustion stability characteristics and proven design. Since limited information is available with oxygen and methane, a test program started with the objective of expanding the design database of a pintle injector through investigation of the effects of atomizer geometric variation on combustion efficiency. On the basis of single-point runs and the use of a segmented calorimetric combustion chamber, four different pintle injector geometries were evaluated. Characteristic velocity efficiency is presented in terms of chamber mixture ratio, injection momentum- and velocity ratios. It is expected that these results will ultimately serve as a yardstick for subsequent fully-throttlable injector developments.

1. Introduction

Thrust modulation of liquid rocket engines is sought after in a variety of mission profiles such as:

- During orbit manoeuvres including orientation and stabilization;

- In space rendezvous and docking;

- For hovering and landing on the surface of celestial bodies;

- In ballistic missile trajectory control.

Throttling ranges are dictated by the particular mission requirements, with higher ratios being adopted where a precise trajectory control is needed. Ratios bellow 4:1 (i.e. 25% of rated thrust level) are usually considered "shallow throttle", requiring simpler techniques for propellant regulation. Contrary to typical space-storable propellants, liquid oxygen and liquid methane are attractive candidates for future space missions, due to their good handling and low-toxicity characteristics. Besides, in comparison with liquid hydrogen, liquid methane provides a superior bulk density in combination with liquid oxygen and can be more easily stored in space, due to its higher boiling point. However, the low heat capacity of liquid methane virtually precludes its use as a coolant below the critical pressure of 45,8 [MPa], where undesirable effects of boiling heat transfer exist.

Aside from the problems of turbomachinery and thrust chamber thermal control, knowledge of the processes involved in the atomization and mixing of propellants in the entire thrust range is necessary to obtain optimum performance and stability [6]. Selection of the proper injection scheme is complicated by the fact that the role of the injector is directly connected with propulsion system performance requirements, combustion stability and chamber-wall heat transfer characteristics. The physical arrangement of the various injection schemes that have been utilized for rocket engine throttling has near-unlimited variety[2], but one of the most popular injection schemes for obtaining reasonable mixing and distribution consists of one or more streams impinging at a common point. The pintle injector, known for

its use in the Apollo Moon missions[3, 4], can be seen as a particular case of a multiple orifice impinging injector. Simplicity in design and construction of such injectors, together with positive control of propellant mass flowrate, accounts for the general acceptance of this basic design whenever thrust modulation is required. The probability that information on pintle injectors using liquid oxygen and liquid methane propellants would most likely help expand the design database and the necessity for some restriction on the scope of the experimental tests resulted in this investigation of the geometric effect of pintle injectors in engine performance.

2. Overview of Pintle Injector Design

The pintle injector design is fundamentally based upon obtaining a mechanical interlock of the propellants, which forces liquid phase mixing to occur. Selection of a oxidizer-centered or fuel-centered pintle design can be established in terms of propellant combination and thrust level. One design criterium establishes that for thrust levels above approximately 5000 [N] [1] the oxidizer is employed as the center propellant in a pintle injector. The oxidizer is metered and directed radially outward as individual streams from the central pintle. The fuel is injected as a hollow cylindrical sheet which intercepts the oxidizer streams, with part of the fuel impinging the oxidizer and part of it penetrating between the oxidizer orifices. The injection parameters for this type of injector which showed a dominating influence on injector performance [10] are as follows:

1. Ratio of oxidizer to fuel injection momentum (*TMR*);

2. Ratio of secondary oxidizer flow to primary orifice flow, if any;

3. Number, size and shape of oxidizer orifices;

4. Elemental spacing of oxidizer orifices;

5. Location of secondary oxidizer orifices;

6. Injection pressure level and mixture ratio.

Variation of these parameters are used to control both performance and wall environment. As a part of the design analysis, the effects of geometry, momentum and velocity ratios, impingement angles and pressure drops were then studied. The results of these analyses was finally used to establish all of the injector dimensions. By considering initially the continuity equation and liquid injection at an average temperature of 120 [K] and the flow area-pressure relationship we obtain:

$$C_d A = \left[\frac{\dot{m}}{2\rho \Delta P} \right]^{1/2}. \tag{1}$$

where C_d is the average discharge coefficient, A is the flow area, $\dot{m}$ is the propellant mass flow rate and ΔP is the pressure drop across the element. It is found from Equation (1) that the propellant injection area requirements are small for a 500-[N] thruster. However, the area is a function of the orifice pressure drops selected, and this parameter must be optimized with the oxidizer pressure drop to result in optimum mixing performance. The hydraulic factor involving momentum ratios is a measure of the inherent propellant energy for atomization and mixing. From first principles, this ratio is represented as [8]:

$$\frac{F_f}{F_o} = \frac{\dot{m}_f V_f}{\dot{m}_o V_o}. \tag{2}$$

F_f is the fuel force on the oxidizer, F_o is the oxidizer force on the fuel, $\dot{m}_f$ is the fuel mass flowrate, $\dot{m}_o$ is the oxidizer mass flowrate, V_f and V_o are the respective fuel and oxidizer injection velocities. To assure that peak performance can occur virtually through all throttling range, it is necessary to optimize the injector hydraulics. A study conducted by Rupe [7] revealed that control of basic propellant momentum results in peak performance. Behind this statement lies the assumption than an optimum reaction predicates intimate physical mixing on a molecular level and in the correct proportions for a stoichiometric and/or more favourable reaction. In the ideal case this condition would exist immediately after injection. The reaction time (or rather the mixing time) would approach a minimum, and combustion chamber volume could then be reduced to an optimum size. This criteria is especially applicable in either case of sheet or jet injectors. According to Rupe [7] sheet types of one-on-one elements should perform best for:

$$\left(\frac{\rho_1 V_1^2}{\rho_2 V_2^2} \right) \left(\frac{d_1}{d_2} \right) \approx K. \tag{3}$$

EFFECT OF PINTLE INJECTOR GEOMETRY ON COMBUSTION IN A LOX/LCH$_4$ ROCKET ENGINE

or in terms of mixture ratio:

$$K_m^2 \frac{\rho_f}{\rho_o} \left(\frac{d_f}{d_o} \right)^3 \approx K. \tag{4}$$

where K_m is the mixture ratio, ρ_f and ρ_o are the fuel and oxidizer densities upon injection, respectively, and K is a constant. A simple but effective approach to this control is obtained through an examination of the gross dynamics of interaction of fuel and oxidizer, as follows:

- Initial maximum mixing can be achieved only by optimum use of available momentum forces (the product of density and area times the square of the velocity);

- If the oxidizer is not injected as a continuous film, the fuel sheet intercepts the oxidizer streams, part of the fuel striking the top surface and part of it dropping in between the oxidizer slots. It is assumed that the reaction products contribute to drive the propellants into each other;

- For the single-element injector configuration, the proper areas for the fuel and oxidizer are obtained through an examination of the initial interaction mechanics. Assuming that the oxidizer is injected in the center and the fuel is injected as a continuous annular sheet, the following interaction model is proposed:

$$F_f = \rho_f V_f^2 \left[tW + tLC \right]. \tag{5}$$

where W and L are the width an height of the central orifices, t is the annular sheet thickness and C is a cross-influence term to account for the side interaction of the fuel on the oxidizer. On the basis of a single interaction between elements for a fuel particle a first approximation to C is given as:

$$C = \left(\frac{L}{V_f} \right) \left(\frac{a}{S} \right) \left[1 - \left(\frac{NS}{\pi D_{fm}} \right) \right].$$

which is seen to be an estimate of the ratio of time of flight of the fuel to the dispersion of the two-phase reactants. The value of a, which is a measure of the velocity of a disturbance, is taken as that of a nearly homogeneous two-phase mixture. Here, S is the distance between adjacent orifices and D_{fm} the diameter relating to annular sheet injection point. The oxidizer force on the fuel is given by:

$$F_o = \rho_o V_o^2 WL. \tag{6}$$

Therefore, the final momentum ratio of the slot configuration is:

$$\frac{F_f}{F_o} = \frac{\rho_f V_f^2 t \left[W + 2LC \right]}{\rho_o V_o^2 WL}. \tag{7}$$

According to Yang et al. [10], the final momentum ratio result for optimal momentum utilization becomes:

$$\frac{\rho_f V_f^2 \left[tW + 2tLC \right]}{\rho_o V_o^2 WL} = 1. \tag{8}$$

Similarly, for a single row of circular orifices, the fuel force on the oxizider is:

$$F_f = \rho_f V_f^2 td. \tag{9}$$

where d is the radial orifice diameter. The force of the oxidizer acting on the fuel is:

$$F_o = \rho_o V_o^2 \frac{\pi d^2}{4}. \tag{10}$$

Leading to an optimum momentum utilization given by

$$\frac{\rho_f V_f^2 td}{\rho_o V_o^2 \frac{\pi d^2}{4}} = 1. \tag{11}$$

Pintle injector designs based upon these underlying principles provide peak performance at the optimum momentum ratios as defined by Equations (8) and (11). Table 1 summarizes pintle injector design information.

EFFECT OF PINTLE INJECTOR GEOMETRY ON COMBUSTION IN A LOX/LCH₄ ROCKET ENGINE

Table 1: Summary of pintle injector design.

LOX massflow, $[\frac{kg}{s}]$	0,085
LCH$_4$ massflow, $[\frac{kg}{s}]$	0,030
LOX injector nominal pressure drop, [MPa]	0,18
LCH$_4$ injector nominal pressure drop, [MPa]	0,60
Number of primary orifices, [-]	12
Orifice aspect ratio (length/width), [-]	2
Blockage factor [10] BF, [-]	0,34
Chamber-to-pintle diameter ratio, [-]	7,15
Skip distance (baseline version), [-]	1,0

2.1 Injector Mechanical Design

At the outset of the design effort, a goal was established to evolve a configuration which would incorporate maximum flexibility as well as economy in fabrication. The injector selected for this purpose was a building block version with replaceable injection elements, which allowed injector modifications with a minimum of schedule impact, see Figure 1. The basic injector concept permits adjusting both the fuel and oxidizer injection flow areas, either separately or simultaneously, thus providing increased flexibility during the initial screening phase. Additionally, this feature allowed a more rapid injector optimization and prevented the use of complex actuating systems, which can be eventually embodied through slight hardware modification. Figure 2 shows the final injector hardware.
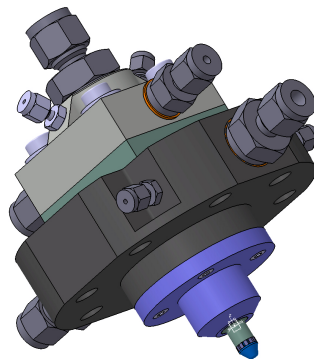

Figure 1: 3-D view of pintle injector.

3. Experimental Apparatus

3.1 Calorimetric Combustion Chamber

For evaluation of the injector types and screening of design configurations, short-duration firings using a calorimetric combustion chamber and nozzle were performed. The nominal design parameters were a throat diameter of 13,5 [mm] and a contraction ratio of 13 with a characteristic chamber length L^* of 1,45 [m]. The nominal mixture ratio of 2,8 is the result of a conceptual trade-off study between performance and fuel availability for chamber cooling. Chamber pressures of $1,0$ to $1,5$ [MPa] were adopted and represent the range typical to pressure-fed thruster applications.

3.2 Ignition System

A conventional torch igniter running on gaseous oxygen and gaseous methane was designed and employed throughout the test-firings. Nominal chamber pressure was 0,35 [MPa] at a mixture ratio of 2,5. Igniter operating times varied during the tests. An average 0,600 [ms] operating time proved sufficient for the majority of main engine mixture ratios investigated.
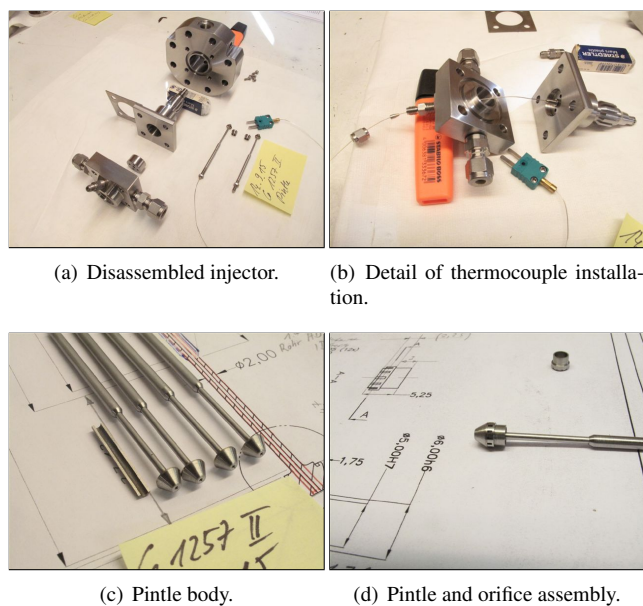
EFFECT OF PINTLE INJECTOR GEOMETRY ON COMBUSTION IN A LOX/LCH$_4$ ROCKET ENGINE

(a) Disassembled injector.

(b) Detail of thermocouple installation.

(c) Pintle body.

(d) Pintle and orifice assembly.
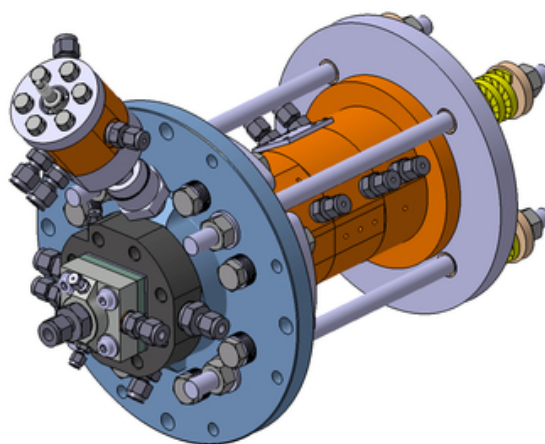
Figure 2: Pintle injector hardware.

Figure 3: 3-D aft view of "workhorse" combustion chamber showing injector and torch igniter mounting.

4. Cryogenic Test Stand

A full description of the cryogenic test bench used in the hot-fire experiments is given by Vasques and Haidn [9]. Production of liquid methane made use of a pressurized liquid nitrogen bath at ca. 0,65 [MPa] to prevent outlet propellant temperatures to drop to or below methane freezing point. Liquid oxygen was produced on-site by direct liquefaction of gaseous oxygen flowing through a stainless steel tubing coil immersed in a liquid nitrogen bath. Both propellant supplies from the liquefier to the main valve used a partially vacuum-insulated, LN$_2$-cooled jacketed line. Propellant flowrates were measured using subcritical venturi meters designed as a three-wall stainless-steel unit allowing a continuous flow of LN$_2$ through the inner annular passage and a vacuum to be maintained in the outer annulus. The liquid nitrogen refrigerant flow was maintained throughout the jacket passages in the flowmeter segment with a final propellant line run from the main valves leading to the engine being simply foam-insulated for simplicity and to improve thrust measurement accuracy.

EFFECT OF PINTLE INJECTOR GEOMETRY ON COMBUSTION IN A LOX/LCH$_4$ ROCKET ENGINE

5. Data Reduction Procedures

5.1 Combustion Efficiency Computation

The index of injector performance used in this study was the corrected combustion efficiency. The correction is necessary inasmuch as it isolates the effects of mixing and vaporization, the two factors of more relevance in injector performance evaluation. By assuming initially a perfect injector, the efficiency attributed to a particular injector design will be:

$$\eta_{C^*} = \frac{C^*_{exp}}{C^*_{idealinj}}. \tag{12}$$

where $C^*_{idealinj}$ is the characteristic velocity that would be obtained with a perfect injector. This value equals the theoretical equilibrium characteristic velocity corrected for effects of throat geometry, chemical kinetics, boundary layer and chamber heat losses. Two independent methods were used for calculating the experimental characteristic velocity C^*_{exp}: (1) based on measurement of chamber pressure and (2) based on measurement of thrust.

5.1.1 Chamber Pressure Method

Characteristic velocity efficiency based on chamber pressure is defined by the following:

$$\eta_{C^*} = \frac{(p_k)_o\,(A_t)_{eff}}{\dot{m}_T\,C^*_{theo}}. \tag{13}$$

where $(p_k)_o$ is the throat stagnation pressure, $(A_t)_{eff}$ the effective nozzle throat area and $\dot{m}_T$ the total propellant mass flowrate. As mentioned previously, values obtained via Equation (13) are referred to as corrected characteristic velocity efficiencies, because the factors involved are obtained by application of suitable influence factor corrections to measured quantities. Stagnation pressure at the throat is obtained from measured static pressure at start of nozzle convergence by assumption of isentropic expansion. Effective throat area is estimated from pre- and post-firing throat diameter measurements and account for non-unity nozzle discharge coefficient. Chamber pressure can be corrected to allow for energy losses from combustion gases to the chamber wall by heat transfer and friction. Equation (13) may therefore be written as follows:

$$\eta_{C^*} = \frac{p_k A_t f_p f_{TR} f_{DIS} f_{FR} f_{HL} f_{KE}}{\left(\dot{m}_o + \dot{m}_f\right) C^*_{theo}}. \tag{14}$$

where the terms f_i are correction factors accounting for pressure at the throat, throat area change, effective throat discharge coefficient and heat and kinetic reaction losses, respectively. C^*_{theo} is simply the theoretical characteristic velocity obtained from equilibrium reactions.

5.1.2 Calculations Based on Thrust

The alternate determination of characteristic velocity efficiency is based on thrust:

$$\eta_{C^*} = \frac{F_{vac}}{\dot{m}_T\,(C_F)_{vac}\,C^*_{theo}}. \tag{15}$$

where F_{vac} is the vacuum thrust and $(C_F)_{vac}$ is the corresponding thrust coefficient. Values of vacuum thrust are obtained by correcting the sea-level measurements. These corrected values can then be used in conjunction with theoretical thrust coefficients for calculation of C^*. Nozzle efficiency is taken as 100% if there is no combustion in the nozzle, if chemical equilibrium is maintained in the expansion process and if energy losses from the combustion gases are taken into account [5].

$$\eta_{C^*} = \frac{(F + p_a A_e)\,\phi_{FR}\phi_{DIV}\phi_{HL}\phi_{KE}}{\left(\dot{m}_o + \dot{m}_f\right)(C_F)_{theo}\,C^*_{theo}}. \tag{16}$$

where F is the measured value of the thrust at sea-level conditions, p_a is the ambient pressure, A_e the nozzle exit area. The ϕ_i terms are correction factors related to chamber-wall frictional and nozzle divergent losses, heat exchange from the combustion gases to the wall and kinetic (non-equilibrium) losses. In Equation (16), the correction factors are directly applied to vacuum thrust rather than the measured thrust, because, for convenience, the factors are readily

6

calculated as changes in efficiency based on theoretical vacuum parameters. Implicit in the use of theoretical C_F values are corrections to geometric throat area and to measured static chamber pressure at the start of nozzle convergence. Therefore, calculation of corrected C^* efficiency from thrust measurement includes all factors of Equation (16) plus an additional one to account for non-parallel nozzle exit flow. Because $(C_F)_{theo}$ is essentially independent of small changes to chamber pressure and contraction ratio which are involved in corrections to p_k and A_t, these corrections are of no practical significance in calculation of C^* from thrust measurements. Methods of estimation of the various correction factors are described in the CPIA Publication 245[5].

6. Experimental Approach

6.1 Injector Configurations Tested

The primary goal of the hot-firing investigation was oriented towards evaluating the performance characteristics of a given injector configuration. However, it also aimed at mitigating, by proper design, the excessive thermal load to the pintle tip observed in early test runs. The pintle tip, manufactured initially of stainless steel, exhibited very low resistance to corrosion originating from the hot, oxidizer rich recirculating streams impinging back on the material. Later replacement of the pintle body material for a copper alloy improved reliability slightly, but proved to be far from a final solution as soon as chamber pressure was increased in subsequent tests and failure was once again experienced. Various approches to circumvent this problem were considered, including:

- Shortening of the tip and oxidizer sleeve from the baseline skip ratio of 1,0 down to 0,5;

- Application of a ceramic coating to the tip material;

- Use of active cooling for the tip by flowing a fraction of the liquid oxygen through the pintle tip axis. This would potentially displace the zone of oxygen-rich recirculation downstream of the tip;

- Inclusion of a ramp to deflect the fuel annular flow, moving the impingement point from the central combustion zone;

- A combination of the afore mentioned approaches.

Of all the potential solutions described, only the ceramic-coated tip was not attempted since no guarantee could be given as to the long-term resistance of the ceramic material at both cryogenic and combustion temperatures. A summary of injector configurations tested is presented in Table 2.

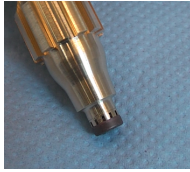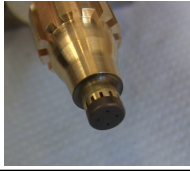## 6.2 Cold-flow Evaluation of Injector Designs

Cold-flow tests had a dual purpose: first to get a qualitative view of the spray patterns and second to measure the spray angles and discharge coefficients of the liquid oxygen and liquid methane injectors. Additionally, these tests provided an indication of the atomization quality, relevant to subsequent hot-fire evaluation of injector candidates. Figure 4 presents the aspect of the spray for Injector 1, which had a shortened pintle length (reduced skip ratio) with respect to the baseline version. The characteristic convergent annular LCH$_4$ flow is depicted in Figure 4(a). Uniform flow conditions through the 0,20-[mm] fuel gap are achieved primarily by use of flow straighteners upstream of the injection point and by careful centering of the LOX sleeve. Figure 4(b) illustrates the combined LOX and LCH$_4$ sprays at optimum momenta. Adjusting the momentum ratio with water to reflect real propellant conditions require conversion of simulant water flows into propellant flow as described by Sutton and Biblarz [8].

Following cold-flow evaluation of Injector 1, the hydraulic characteristics of Injector 2 were established. In reality, these differed only by inclusion of four, 0,5-[mm] holes bored to the pintle tip and parallel to chamber center line (for simplicity, no impingement between jets was implemented), see Figure 5. These orifices should meter the LOX cooling flow to approximately 10% of the total oxidizer mass flowrate. In this case, due to the lower oxidizer velocity though the original radial orifices, a correction in LCH$_4$ gap or re-size of LOX orifices was necessary to guarantee optimum propellant interaction.

Injector 3 included a ramp that deflected the LCH$_4$ annular flow away from the pintle tip, while still retaining the original baseline injector skip ratio, see Figure 6(c). These was primarily aimed at removing the combustion zone from the chamber center, hopefully attenuating pintle tip overheat and throat erosion. The ramp had a 25° deflection angle and resulted in a minor loss in fuel flow momentum. However, this was considered negligible and no correction in the fuel flow gap or LOX orifice flow area was made. Injector 4 combined the ramp solution and additionally the

EFFECT OF PINTLE INJECTOR GEOMETRY ON COMBUSTION IN A LOX/LCH$_4$ ROCKET ENGINE

Table 2: Injector Configurations Evaluated.

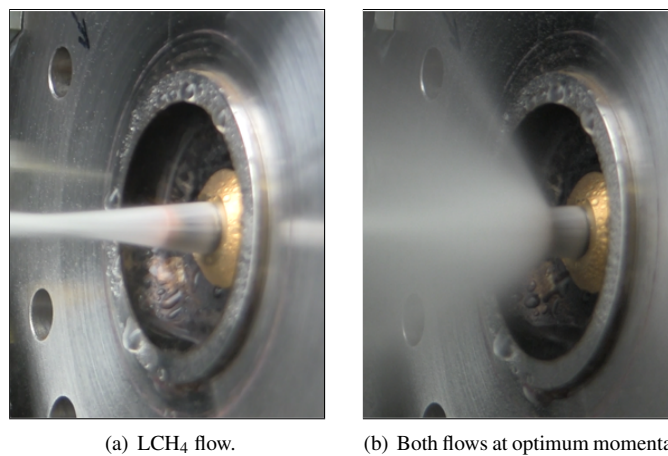| Injector	Description	Figure
1	Shortened LOX passage and reduced skip ratio	
2	Same as injector 1, incorporates active cooling of the pintle tip	
3	Use of a LCH$_4$ deflector for displacement of the impingement point	
4	Same as injector 2, but with a cooled pintle tip	

(a) LCH$_4$ flow.

(b) Both flows at optimum momenta.

Figure 4: Spray patterns for Injector 1.

active cooling of the tip. The introduction of tip cooling in Injector 4 was indeed not necessary as would be proven by subsequent hot-fire tests. As seen in Figure 6(b), the axial cooling flow offers very little opportunity for propellant interaction downstream of the tip. The decay in performance seems to be, in principle, not apparent, as discussed later in Section 6.3.

6.3 Hot-Fire Testing

All hot-fire tests were performed at the rocket test facility of the Faculty of Space Propulsion in Garching, Germany. Typical pressure traces are shown in Figure 7. Although sub-cooled propellant conditions were present upstream of both venturis, measured propellant temperatures and pressures at the injection head were in fact representative of a gas-liquid injection pattern. Liquid oxygen was delivered at near-nominal temperature conditions (circa 90 [K]) while methane transitioned from a saturated state and reached temperatures as high as 180 [K] upon injection. Since one
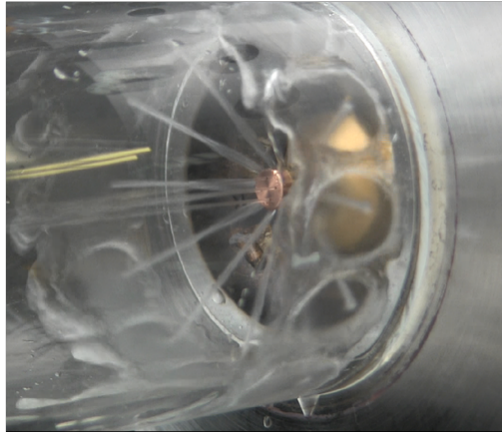
EFFECT OF PINTLE INJECTOR GEOMETRY ON COMBUSTION IN A LOX/LCH$_4$ ROCKET ENGINE

Figure 5: Cold-flow evaluation of Injector 2, showing cooling and primary radial flows.

(a) LOX flow, no tip cooling.

(b) LOX flow with tip cooling.

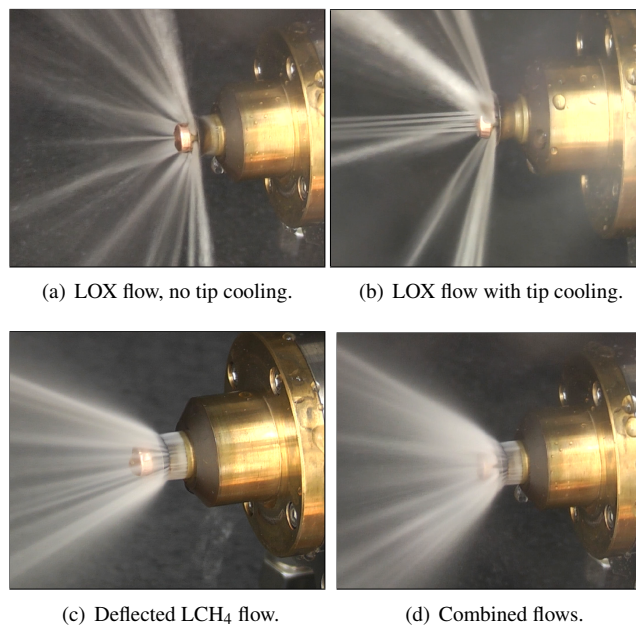(c) Deflected LCH$_4$ flow.

(d) Combined flows.

Figure 6: Water flow-checks with Injectors 3 and 4, with deflected LCH$_4$ flow and two different LOX patterns.

would most likely operate the engine in a regeneratively-cooled mode, this injection condition is justified. Figure 8 shows the typical blueish-colored flame during a test-run.

6.3.1 Instrumentation and Controls

The pressure transducers used were mainly thin-film strain gage instruments and where oxygen compatibility was required, ceramic strain gage transducers were adopted. The load-cell used for thrust measurements was a bonded strain-type transducer with a 1000 [N] rating. This load-cell was selected to provide a high-stiffness and, thus, to result in a high thrust mesasurement response. The cryogenic range temperature measurements were made with copper/constantan (propellant tanks) and chromel/alumel (feed-system) thermocouples by use of feed-throughs or standard connectors. Elevated temperatures, such as those exhibited by the chamber surfaces during firing, were recorded with iron/constantan thermocouples. These were of the bare wire type with stripped leads for faster response. Inner-wall, transient temperature data, used 0,5 [mm]-diameter probe chromel/alumel thermocouples. The propellant flowrates were measured using subcritical venturi meters specially designed for this purpose. A three-wall stainless-steel construction was conceived to permit a continuous flow of LN$_2$ through the inner annular passage, while a vacuum was maintained in the outer annulus for superior thermal insulation. Upstream and downstream of the venturi meters, two mounting blocks were attached. These fully instrumented blocks served as a manifold for the LN$_2$ refrigerant flow and provided interface to all bypass, relief, isolation and main engine valves. Valve actuation as well as chamber start-
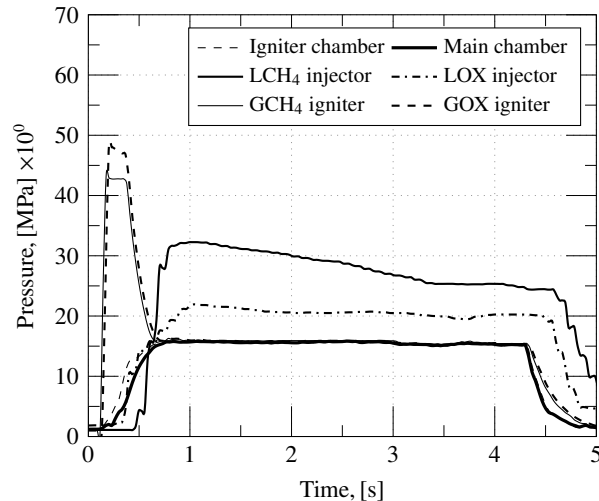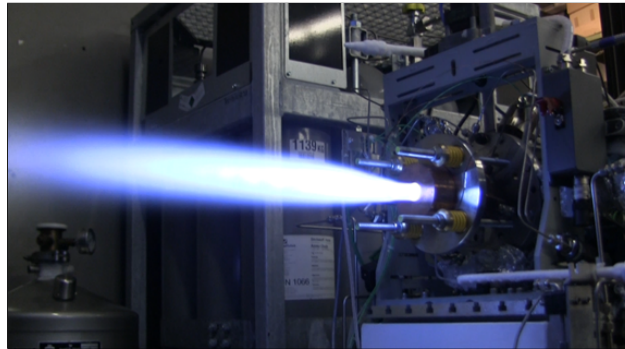
Figure 7: Representative pressure traces.

Figure 8: Hot-fire test run.

and shut-down logics were implemented in conjunction with a Programmable Logic Controller (PLC). Manual and automatic actuation modes could be executed by selecting the appropriate switch position. A manual abort switch that could override any previous logic inputs was available to the operator. Any firing could also be automatically aborted by any of the redline input signals. Dedicated card modules were used for data acquisition at 160 [ksamples/s] and 14 bit resolution.

7. Results and Discussion

7.1 Injector Evaluation

The calculation of characteristic exhaust velocity followed by the chamber pressure method and the C^* efficiency was calculated as indicated in Section 5. The final precision in η_{C*} was $\pm 4,5\%$ for one standard deviation.

Limited performance of Injectors 1 and 2 at 1,5 [MPa] chamber pressure is given in Figure 9. Injector 1 made use of a reduced skip ratio, in an attempt to remove the injector from the core of the combustion zone. This action solely could not prevent failure of the pintle material and tests with Injector 1 were terminated. As a result, a cooled-tip was introduced for Injector 2. The latter provided improved injector durability, as well as enhanced ignition characteristics, possibly due to the axial pattern of LOX cooling streams interacting with the more fuel-rich torch igniter flame. Cooling the tip, however, was no panacea to the overheat problem and degradation of the material resulted after several test runs, preventing any subsequent assessment of Injector 2. Performance at the nominal engine mixture ratio of 2,8, was around $\eta_{C*} = 92,5$ percent for both injector configurations. The characteristic velocity efficiencies of Injectors 1 and 2 as a function of injection momentum and velocity ratios are given in Figure 10. For the propellant injection conditions encountered, oxidizer-fuel momentum ratios lie well below unit, with performance increasing and apparently reaching a maximum around the value of 0,10 (corresponding to a velocity ratio of 0,040) for both injectors.
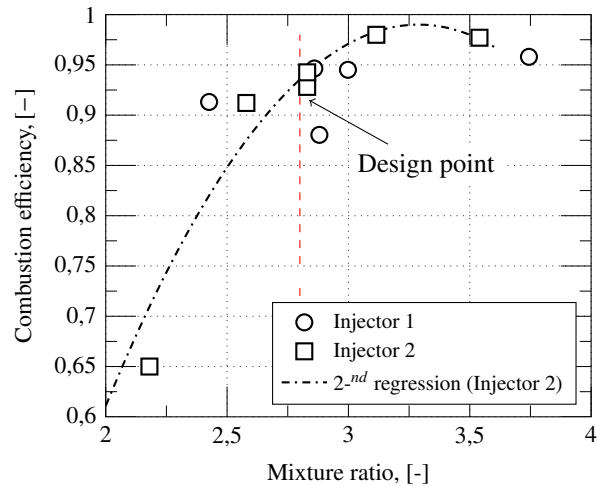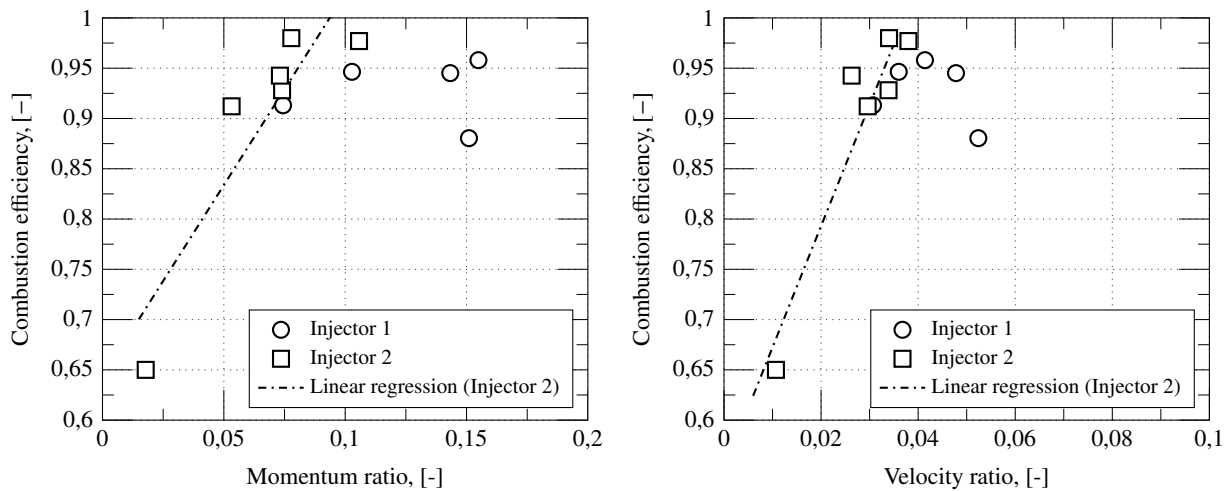
EFFECT OF PINTLE INJECTOR GEOMETRY ON COMBUSTION IN A LOX/LCH$_4$ ROCKET ENGINE

Figure 9: Corrected efficiency η_{C*} for Injectors 1 and 2 (see text).

Figure 10: Trend in characteristic velocity efficiency for Injectors 1 and 2 as a function of oxidizer-to-fuel momentum- and velocity-ratios.

Figure 11 gives the η_{C*} of Injectors 3 and 4 at 1,0 [MPa] chamber pressure as a function of the chamber global mixture ratio. Included in Figure 11 are the computed values of η_{C*} obtained via chamber pressure and thrust measurements, as described in Sections and . Correction of the mixture ratio for Injector 4 to reflect the conditions of the interacting sprays only, is given in Figure 12. Although the cooling flow did not participate directly in the initial interaction process, it was felt that correction in η_{C*} was not necessary. The intense central recirculation fan, characteristic of pintle injectors, leads the cooling flow to mix downstream of the injection point, ultimately contributing to chamber pressure build-up and thrust generation. According to Figure 12, both injectors were 83 percent efficient at the design point. As shown in Figure 13 for Injector 4, performance increases with momentum ratio and reaches a peak at 0,20 (or around 0,045 in terms of velocity ratio). These figures represent a trend, since not enough data is available to envelope the complete spectrum of injection velocities.

The introduction of the ramp definitely solved the overheat issue by moving the combustion zone away from the tip. Injectors 1 and 2 had improved performance, however. The reason for this is problably the decelerating effect the ramp created in the flow of fuel. This resulted in non-uniform momentum exchange with zones where propellant did not ideally react. The fuel deflector occasionally created ignition difficulties and although a perfectly suitable explanation for this anomaly has not been devised, it is possible that for some injection conditions the flame could not be properly anchored.
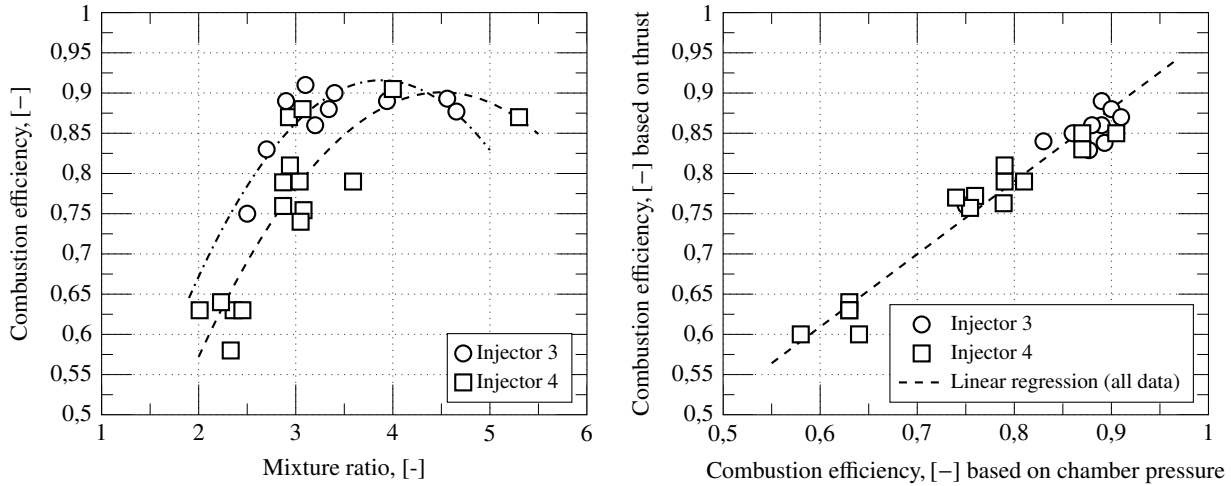
EFFECT OF PINTLE INJECTOR GEOMETRY ON COMBUSTION IN A LOX/LCH₄ ROCKET ENGINE

Figure 11: Overall performance for Injectors 3 and 4 and comparison of thrust- and chamber pressure-based methods of η_{C^*} computation.
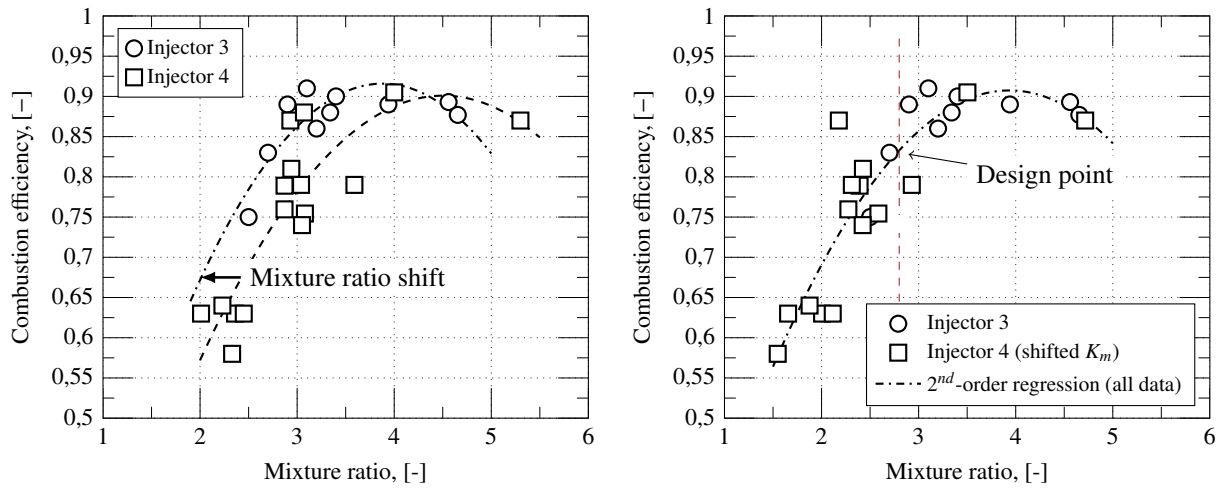

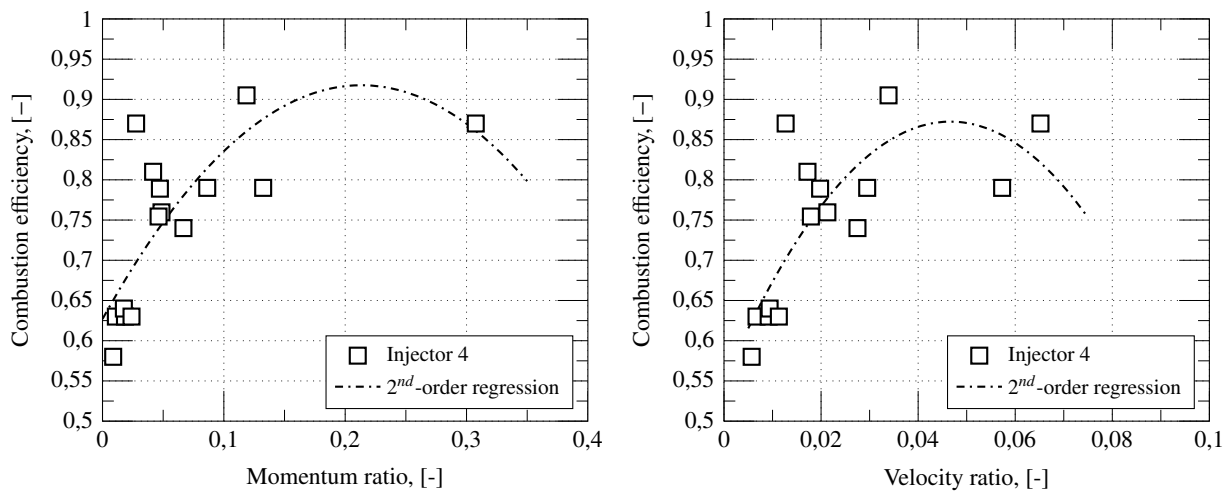Figure 12: Corrected performance of Injector 4 to account for LOX flow tip cooling.

Figure 13: Combustion efficiency for Injector 4 as a function of oxidizer-to-fuel momentum- and velocity-ratios.

8. Conclusions

Performance evaluation of four different pintle injector configurations were presented in terms of injection momentum and velocity ratios. The results can be summarized as follows:

1) The first configuration had a reduced skip ratio with respect to the baseline version and no pintle tip cooling. Performance data at the nominal mixture ratio indicated values around 92,5 percent. Tests were terminated resulting from failure of the pintle tip due to overheat;

2) A second injector was identical to the first configuration, except that it incorporated an actively-cooled pintle tip. Cooling was effected by flowing 10% of the LOX-flow through four, 0,5-[mm] holes bored in the tip. Tests at 1,5 [MPa] resulted in similar combustion efficiency around the nominal mixture ratio as Injector 1 and improved ignition characteristics. After several firings, the pintle material failed structurally;

3) Deflection of the methane flow out of the pintle tip region, forcing impingement outside of the central combustion chamber zone, considerably enhanced pintle tip life and reduced throat erosion at the cost of lower performance. At a chamber pressure of 1,0 [MPa] this modified injector had a combustion efficiency of 83 percent around the nominal mixture ratio. In order to assess the influence of tip cooling with the presence of the ramp, a fourth configuration was tested. These tests indicated no considerable influence of additional pintle cooling in the characteristic velocity efficiency;

4) Values of combustion efficiency in terms of momentum and velocity ratio were presented for all injectors, although in limited form for the first and second configurations. Due to the gas-liquid injection conditions observed, an oxidizer-to-fuel momentum ratio between 0,1 and 0,2 was required to maximize performance. A corresponding velocity ratio of 0,04 to 0,05 is needed. Whereas the controlling parameter could be momentum rather than velocity, the information available does not warrant any distinction;

5) Although not investigated, there is sufficient reason to believe that through adequate design of the deflector, an improvement in performance and dependable operation can be attained. With the addition of secondary radial orifices and a modified ramp angle, the possibility to organize chamber mixture ratio and related chamber-wall heat transfer characteristics is created.

9. Acknowledgments

References

[1] M. J. Bedard, T. W. Feldman, A. Rettenmaier, and W. Anderson. Student Design/Build/Test of a Throttlable LOX-LCH4 Thrust Chamber. In *48th AIAA/ASME/SAE/ASEE Joint Propulsion Conference & Exhibit*, number AIAA 2012-3883, August 2012.

[2] M. J. Casiano, J. R. Hulka, and V. Yang. Liquid-Propellant Rocket Engine Throttling: A Comprehensive Review. In *45th AIAA/ASME/SAE/ASEE Joint Propulsion Conference & Exhibit*, number AIAA 2009-5135, 2009.

[3] G. Dressler. Summary of Deep Throttling Rocket Engines with Emphasis on Apollo LMDE. In *42nd AIAA/ASME/SAE/ASEE Joint Propulsion Conference & Exhibit*, 2006.

[4] G. Dressler and J. Bauer. TRW pintle engine heritage and performance characteristics. In *36th AIAA/ASME/SAE/ASEE Joint Propulsion Conference and Exhibit*, number AIAA-2000-3871, TRW, Inc., Redondo Beach, CA, July 2000.

[5] K. W. Gross and S. A. Evans. *JANNAF Rocket Engine Performance Test Data Acquisition and Interpretation Manual*, 1975.

[6] T. D. Harrje. *Liquid Propellant Rocket Combustion Instability*. Number NASA SP-194 in Special Publication. Scientific and Technical Information Office, Cleveland, Ohio, January 1972.

[7] J. Rupe. On The Dynamic Characteristics of Free Liquid Jets and a Partial Correlation with Orifice Geometry. Technical Report 32-207, Jet Propulsion Laboratory, Pasadena, California, 1962.

[8] G. P. Sutton and O. Biblarz. *Rocket Propulsion Elements*. Wiley, Hoboken, NJ, 7th edition, 2001.

[9] B. Vasques and O. Haidn. Uncertainty Analysis as Applicable to a Miniature Cryogenic Test Stand for Rocket Research. In *31st International Symposium on Space Technology and Science*, 2017.

[10] V. Yang, M. Habiballah, J. Hulka, and M. Popp. *Liquid Rocket Thrust Chambers: Aspects of Modeling, Analysis, and Design*, volume 200, Progress in Astronautics and Aeronautics. American Institute of Aeronautics and Astronautics, Inc., 2004.